Movable Quiet Zones for Permanent Noise Reduction

Sven Höber[1], Christian Pape[1], Eduard Reithmeier[1]
[1] Institut für Mess- und Regelungstechnik, Leibniz Universität Hannover, 30167 Hannover, Germany
Email: sven.hoeber@imr.uni-hannover.de

Abstract

Active noise control (ANC) systems can by now be encountered in numerous applications such as headphones for the consumer but also the professional market. Particularly, at industrial workplaces or open-plan offices, where people are exposed to high and permanent noise levels, ANC could provide a substantial ear protection. However, most available solutions are either designed as devices to be carried all the time or are tailored to specific environments. As part of this contribution, an ANC system is presented that aims to provide a permanent noise level reduction at the ears without requiring headphones or bulky installations. For this, it generates a moving quiet zone (the area of reduced sound pressure) which is automatically tracked in respect of the listener's position by using virtual microphones combined with a camera system. In contrast to the usual stationary quiet zone analyses, this contribution discusses the dynamic noise reduction, i.e. the tracking performance of the quiet zone, by evaluating the noise level at a moving target position.

Introduction

ANC systems aim to reduce air-bound noise by emitting noise of opposite phase, so-called anti-noise. However, when considering large enclosures the original noise level can often be reduced only locally, resulting in spatially limited quiet zones. Naturally, those quiet zones are bound to the location of the physical microphones of the ANC system, which are placed at the desired points of destructive interference with the anti-noise. Hence, they allow for noise reduction at fixed positions only. To generate a quiet zone at a remote and moving location, several works have investigated the incorporation of virtual sensing, i.e. the placement of virtual microphones. By now, various algorithms have been developed for this [1], of which the remote microphone technique (RMT) is widely used in recent virtual sensing-aided ANC applications. It estimates the sound pressure aside from a physical microphones on basis of the respective transfer path models, which have to be identified in a preliminary stage. This way, the quiet zone can be created at the location of the virtual microphone. However, considering a moving target location, e.g. a human listener, the quiet zone and thus the virtual microphone would have to be moved accordingly. For this, Moreau et al. proposed the use of a camera system to continuously track the movement of the listener's head. In [2], Elliott et al. implemented an according tracking system for use with a so-called active headrest, to move the quiet zones at the sitting listener's ears in respect of the head rotation. For this, a number of virtual microphones are placed at predetermined positions within the assumed area of movement. The virtual microphones could then be addressed separately by switching the corresponding models in respect of the estimated position that was provided by the camera.

The ANC system presented in this paper aims at generating a quiet zone around the head of a moving listener, but remote from fixed installations like headrests, to provide freedom of movement like it is desired at various workplaces. Consequently, in contrast to applications where the listener remains close to the anti-noise sources, the transfer paths to the target positions considered here show significant delays. These limit the dynamic behavior of LMS algorithm-adapted ANC systems [3], i.e. the convergence speed of the quiet zone, and additionally vary with the particular target position or its distance to the anti-noise source, respectively. Those aspects are taken into account for an estimation of the quiet zone's tracking performance, which is conducted in this contribution.

Firstly, the following section describes the developed ANC system, illustrating its practical setup in an experimental environment as well as its software implementation. Subsequently, its performance is analyzed in simulations to derive an estimation of the quiet zone's tracking capability in respect of the available parameters. Finally, these results are validated experimentally by considering a moving microphone as the target of the quiet zone.

Setup of the ANC System

The developed ANC system is implemented as a multiple-channel feedforward control and set up inside a $2.8 \times 2.8 \times 2.4\ \mathrm{m}^3$ low-reflection room as depicted in Fig. 1. It comprises two secondary (anti-noise) sources, driven by the signals

$$\mathbf{y}(n) = [y_1(n) \quad y_2(n)]^T, \tag{1}$$

as well as two error microphones that are placed near the sources, providing the error signals

$$\mathbf{e}_{\mathrm{p}}(n) = [e_{\mathrm{p},1}(n) \quad e_{\mathrm{p},2}(n)]^T. \tag{2}$$

Another microphone is placed in front of the loudspeaker that represents the primary (noise) source to obtain a reference signal $x(n)$ of the emitted noise. As can be seen, this setup uses a concentrated and spatially fixed primary source, representing an engine or similar machine. To eventually generate a quiet zone with respect to a moving target within the designated work area (in the lower right quarter of the room), virtual microphones are placed there using the remote microphone technique and a camera system for tracking of the target's position. A block diagram of the corresponding control design is also shown in Fig. 1. Its software implementation, which runs

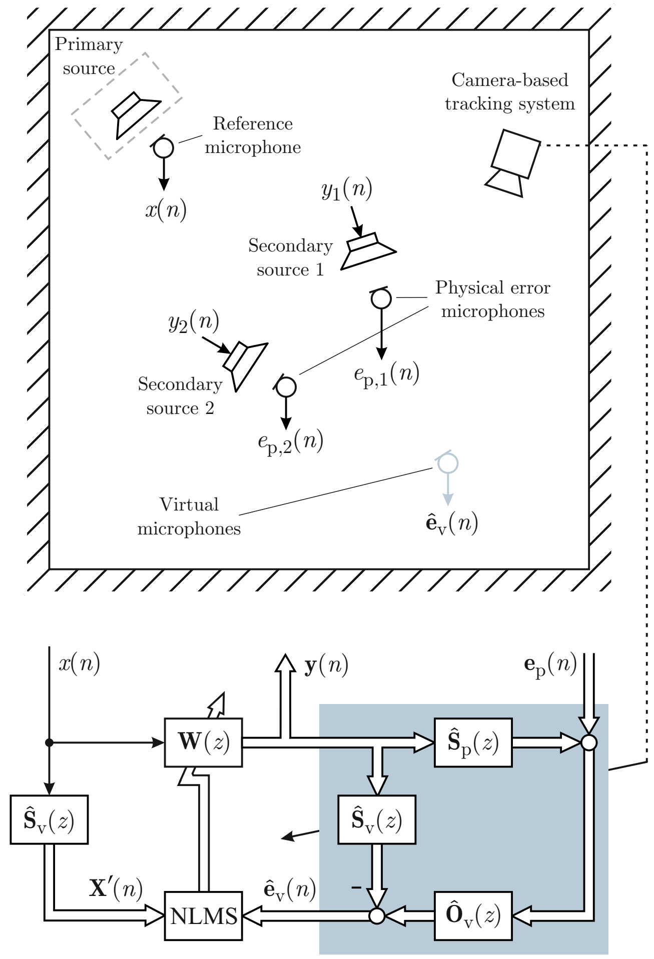

Figure 1: Schematic top view of the ANC system setup inside the low-reflection room and block diagram of its implementation on a digital signal processor platform.

on a remote processor platform, is illustrated briefly in the following (a detailed elaboration on multiple-channel ANC in general can be found in [4], for example).

The optimal driver signals $\mathbf{y}(n)$ for the secondary sources, i.e. the optimal anti-noise, are obtained by filtering the reference signal $x(n)$ with the FIR control filters

$$\mathbf{W}(z) = [W_1(z) \quad W_2(z)]^T. \tag{3}$$

Their coefficient vectors $\underline{\mathbf{w}}(n) = [\mathbf{w}_1(n) \quad \mathbf{w}_2(n)]^T$ of length L are continuously adapted using the well-known FxLMS algorithm according to

$$\underline{\mathbf{w}}(n+1) = \underline{\mathbf{w}}(n) + \frac{\mu_0}{L \cdot \mathbf{x}^T(n)\mathbf{x}(n)} \cdot \mathbf{X}'(n) \cdot \hat{\mathbf{e}}_v(n). \tag{4}$$

Here,

$$\mathbf{x}(n) = [x(n) \quad x(n-1) \quad \cdots \quad x(n-1+L)]^T \tag{5}$$

and

$$\mathbf{X}'(n) = \underline{\hat{\mathbf{S}}_v}^T(n) \otimes \mathbf{x}(n), \tag{6}$$

where the matrix $\underline{\hat{\mathbf{S}}_v}(n)$ contains the coefficient vectors of the secondary path models $\hat{\mathbf{S}}_v(z)$ (corresponding to the virtual microphones) and $\otimes$ denotes the Kronecker product. The algorithm aims to minimize the power of the virtual error signals

$$\hat{\mathbf{e}}_v(n) = [e_{v,1}(n) \quad e_{v,2}(n)]^T, \tag{7}$$

provided by the virtual microphones, both placed at the target location within the area in front of the secondary sources. Eventually, the virtual error signals are estimated on basis of the physical (measured) error signals $\mathbf{e}_p(n)$, using the transfer path models $\hat{\mathbf{S}}_v(z)$, $\hat{\mathbf{S}}_p(z)$ (the secondary paths to the physical microphones) and $\hat{\mathbf{O}}_v(z)$ as depicted in the block diagram (in the lower half of Fig. 1). Usually, these have to be identified in a preliminary stage and are thus only valid for the current setup of sources and sensors. To allow for a movement of the virtual microphones with respect to a moving target at run-time, an algorithm as used in [2] (described in the introduction) is implemented. Accordingly, the virtual microphones are placed at multiple predetermined locations within the designated area of movement for identification of the respective transfer paths. The resulting models are stored in a look-up table (LUT) with correspondence to those locations, so that they can be switched at run-time with respect to the estimated target position provided by the camera.

Considering Eq. (4), the adaptation of the anti-noise, i.e. the convergence of the control filters, is determined by the basic step size μ_0 (actually, the normalized LMS – NLMS – algorithm is used here, where the final step size μ is scaled in respect of the reference signal power represented by the term $L \cdot \mathbf{x}^T(n)\mathbf{x}(n)$). An increase of μ_0 would accelerate the adaptation, but, if exceeding a certain limit, can cause divergence. Consequently, this parameter determines the dynamic behavior of the noise control and that way the movement of the quiet zone, as will be analyzed in the following sections.

Estimation of the Tracking Performance

The adaptive control system is firstly analyzed in simulations to estimate its tracking capability with respect to the basic step size μ_0. For this, a straight horizontal line at a height of 1.6 m is considered within the work area, representing the target's trajectory. Along the trajectory, five fixed positions (i) are chosen, aligned in equal distances of 0.2 m over a range of 0.8 m. Preliminar-

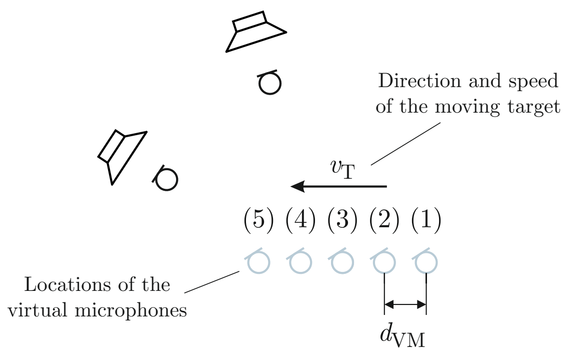

Figure 2: Schematic of the setup for evaluation of the tracking performance: five locations for the virtual microphones, aligned on the straight trajectory of the moving target.

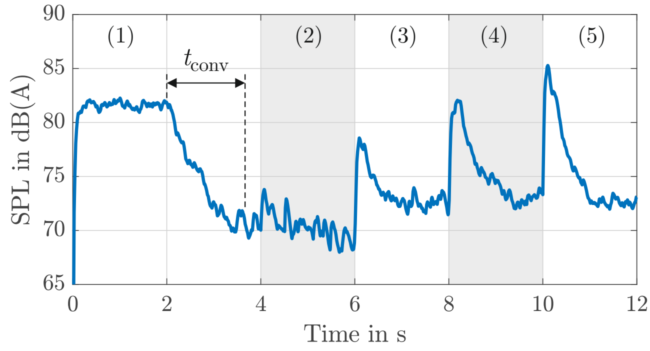

Figure 3: Simulated SPL at the virtual microphones' locations while switching through the respective models (as denoted by the upper numbers) with $\mu_0 = 0.2$.

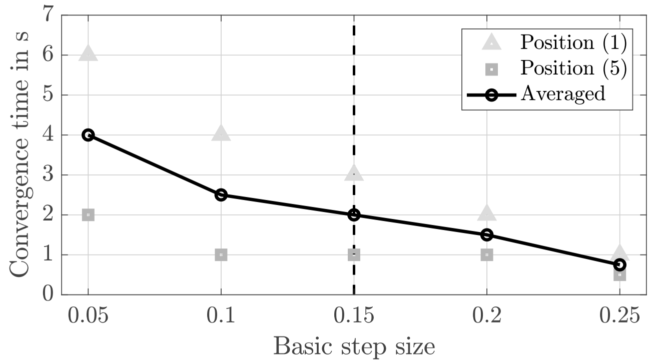

Figure 5: Estimated convergence times at the positions (1) and (5) in respect of the basic step size.

ily, all transfer paths to those positions were measured for use in the control system simulation; its performance will be evaluated in the following by means of the sound pressure level at the fixed positions. According to the moving quiet zone algorithm described before, they also constitute the designated locations of the virtual microphones (see Fig. 2), for which the required models are identified on basis of the measured paths. Eventually, the moving target is simulated by incrementing through the virtual microphones, i.e. changing the corresponding models, every two seconds. All models are FIR filters of length 70, while 180 coefficients are used for the control filters $\mathbf{W}(z)$. The broadband noise to be controlled is represented by band-filtered white noise (featuring a constant power spectrum between $100 - 1000$ Hz).

Using a basic step size of $\mu_0 = 0.2$ at first, Fig. 3 shows the sound pressure level (SPL) that is simulated at the changing target position (denoted by the upper numbers). As can be seen, the target remains at the initial position (1) for the first 4 s. As the control starts after 2 s, the SPL decreases, dropping from 82 dB(A) to about 71 dB(A) on average within approximately 1.8 s. The subsequent change to position (2) causes a further decrease, whereas at the remaining position changes the SPL briefly increases at the respective times (after 6, 8 and 10 s). This is due to the change of the virtual microphone models, after which the anti-noise has to be newly adapted first. As explained before, the adaptation speed is controlled by the basic step size μ_0, which hence influences the decrease of the SPL. This is exemplified in Fig. 4, showing the course of the SPL for the bisected and the quartered value, respectively, of the original basic step size. As can be seen, for each bisection of the step size the SPL decreases slower than before, making the interval of 2 s too short for the SPL to reach the lowest level (as with $\mu_0 = 0.2$). Particularly, at position (1) the final average level, before the position is changed again, increases by about 2 to 3 dB with each bisection. In the following, that dependency is examined further by evaluating the convergence time t_{conv}, which is derived from the approximate time that the SPL takes to remain at an average level after the position was changed. Fig. 5 shows the convergence times for different step sizes at the starting position (1) and the ending position (5) of the trajectory. As expected, the averaged course suggests a general increase of the step size for fastest convergence. However, for some positions within the work area it has shown that the adaptation of the control filters diverges for $\mu_0 > 0.15$. To provide a general estimation of the tracking performance over the entire work area (not only for the considered trajectory), the convergence times for this upper limit constitute the fastest adaptation possible. That is, the target has to remain for at least that time at each position for the quiet zone to fully converge (providing maximum SPL reduction) before moving on to the next position.

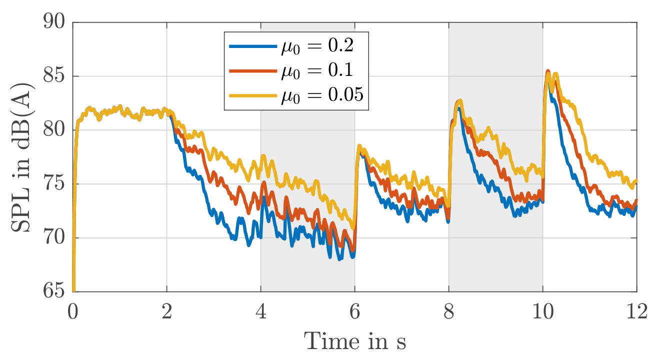

Figure 4: Simulated SPL at the virtual microphones' locations (see Fig. 3) using different step sizes.

Considering the distance d_{VM} of adjacent locations of the virtual microphones, this now allows for an expression of the maximum tracking speed of the quiet zone with respect to the adaptation speed as

$$v_{\mathrm{Q,max}} = \frac{d_{\mathrm{VM}}}{t_{\mathrm{conv}}(\mu_{0,\mathrm{max}})}. \tag{8}$$

Experimental Results

The previously estimated tracking performance of the control system is now validated experimentally, considering the same setup as used for simulation. However, now the required transfer path models are directly identified within the room using the respective program running on the signal processing hardware. On its memory, the models are stored with correspondence to the positions that were provided by the camera.

The moving target is represented by an auxiliary physi-

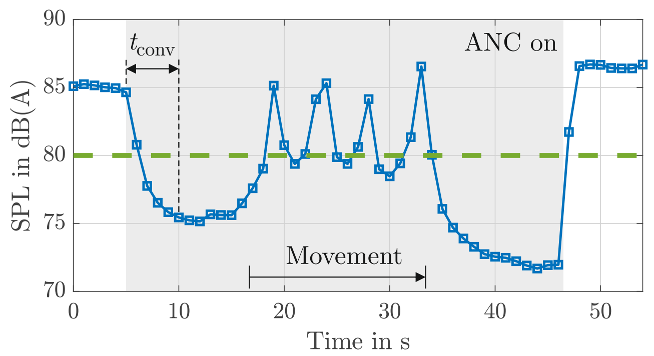

Figure 6: SPL measured by the auxiliary microphone while being moved along the trajectory at a speed of $v_T = 0.055$ m/s. The times before and after movement represent standstill at the position (1) and (5), respectively.

cal microphone that is mounted to a linear drive (located on the ground of the work area) and connected to a remotely placed sound level meter. The linear drive moves the microphone along the known trajectory at a constant speed v_T while it is tracked by the camera. According to its estimated position, the models of the virtual microphones are switched at half the distance to the respective next location $(i+1)$. The SPL that is continuously measured (sampled every second) by the moved microphone is shown in Fig. 6. As can be seen, it first remains at the starting position (1) to provide time for full convergence of the anti-noise (starting after about 5 s), then it is moved to position (5) where the anti-noise is given time again to adapt before the control is turned off. During movement, the SPL clearly shows the changes of the positions by the brief peaks. In between, at the very locations of the virtual microphones, the SPL drops to just below 80 dB(A) (emphasized by the dotted line), whereas at the starting and the ending position it decreases down to 75 or 72 dB(A), respectively. This discrepancy results from the speed of the moving microphone; with $v_T = 0.055$ m/s it exceeds the maximum tracking speed of the quiet zone here, which, according to Eq. (8), yields

$$v_{Q,\max} = \frac{0.2 \text{ m}}{5 \text{ s}} = 0.04 \text{ m/s}. \quad (9)$$

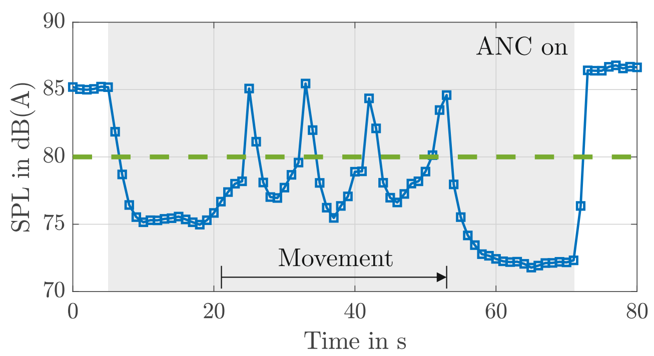

Figure 7: SPL measured by the auxiliary microphone while being moved along the trajectory at a speed of $v_T = 0.027$ m/s.

Consequently, the quiet zone cannot fully converge before the virtual microphone models are switched again. In turn, when the traversing speed v_T is bisected, the SPL decreases rapidly enough to reach levels down to 76 dB, as shown in Fig. 7. Since $v_T < v_{Q,\max}$, the time that the moving microphone remains within the area of each location (i) now suffices for full convergence of the quiet zone – as could be predicted using Eq. (8).

Conclusion and Outlook

In this paper, an ANC system for broadband noise reduction at moving locations was presented and analyzed regarding its tracking performance, i.e. the capability of the generated quiet zone to track a moving target. It was realized as a multiple-channel feedforward control using the FxNLMS algorithm for anti-noise adaptation and the remote microphone technique for implementation of virtual microphones. By dynamically switching between multiple virtual microphones, placed along a moving target's trajectory, the generated quiet zone could be tracked in respect of the target's position, which was continuously estimated by a camera system.

By evaluating the sound pressure level (SPL) reduction at a moving location in simulations, the dynamic behavior of the tracked quiet zone was found to depend on the virtual microphone placement as well as the basic step size of the NLMS algorithm, which controls the anti-noise adaptation. Hence, given a static setup, the latter is the only parameter for tuning the tracking performance of the ANC system. However, in practical application the basic step size is limited, which, in turn, limits the quiet zone's tracking speed. Finally, this was validated in experiments by showing that the SPL at a moving microphone could only be reduced sufficiently if its traversing speed was kept below the estimated tracking speed of the quiet zone.

Since the step size of the NLMS algorithm is eventually limited by the secondary path delays, as mentioned initially (see [3]), the convergence of the quiet zone and thus its tracking speed could be accelerated by using another adaptation algorithm. Also, according to Eq. (8) the tracking speed would be increased by a wider spacing of the virtual microphones' locations, which could be realized by enlarging or interpolating the quiet zone to ensure a covering of the transition areas.

References

[1] Moreau, D., Cazzolato, B., Zander, A., Petersen, C.: A review of virtual sensing algorithms for active noise control. Algorithms (2008), 69-99

[2] Elliott, S. J., Jung, W., Cheer, J.: Head tracking extends local active control of broadband sound to higher frequencies. Scientific Reports (2018), 1-7

[3] Long, G., Ling, F., Proakis, J. G.: The LMS algorithm with delayed coefficient adaptation. IEEE Transactions on Acoustics, Speech, and Signal Processing (1989), 1397-1405

[4] Kuo, S. M., Morgan, D. R.: Active Noise Control Systems: Algorithms and DSP Implementations. John Wiley & Sons, Inc., 1996.